ELSEVIER

Journal of Fluids and Structures 26 (2010) 793–803

JOURNAL OF FLUIDS AND STRUCTURES

www.elsevier.com/locate/jfs

Modification of equation of motion of fluid-conveying pipe for laminar and turbulent flow profiles

C.Q. Guo[a,b,*], C.H. Zhang[a], M.P. Païdoussis[c]

[a]*Department of Hydraulic Engineering, Tsinghua University, Beijing 100084, China*
[b]*School of Mathematics and Physics, University of South China, Hengyang, Hunan 421001, China*
[c]*Department of Mechanical Engineering, McGill University, 817 Sherbrooke Street W., Montreal, QC, Canada H3A 2K6*

Received 25 November 2009; accepted 25 April 2010
Available online 19 June 2010

Abstract

Considering the non-uniformity of the flow velocity distribution in fluid-conveying pipes caused by the viscosity of real fluids, the centrifugal force term in the equation of motion of the pipe is modified for laminar and turbulent flow profiles. The flow-profile-modification factors are found to be 1.333, 1.015–1.040 and 1.035–1.055 for laminar flow in circular pipes, turbulent flow in smooth-wall circular pipes and turbulent flow in rough-wall circular pipes, respectively. The critical flow velocities for divergence in the above-mentioned three cases are found to be 13.4%, 0.74–1.9% and 1.7–2.6%, respectively, *lower* than that with plug flow, while those for flutter are even lower, which could reach 36% for the laminar flow profile. By introducing two new concepts of equivalent flow velocity and equivalent mass, fluid-conveying pipe problems with different flow profiles can be solved with the equation of motion for plug flow.

Keywords: Fluid-conveying pipe; Equation of motion; Critical flow velocity; Laminar flow; Turbulent flow

1. Introduction

The fluid-conveying pipe is a canonical problem in the study of fluid-structure interactions. Since the early works by Ashley and Haviland (1950), Housner (1952), Benjamin (1961a), Gregory and Païdoussis (1966) and Païdoussis and Issid (1974), there are approximately 550 significant publications on this subject, counting up to 2003 (Païdoussis, 2008). As noted by Païdoussis and Li (1993), this has become a ''model dynamical problem'', a new paradigm in dynamics. In its simplest form, the governing equation of motion is simple enough to solve, yet can demonstrate generic features of much more complex dynamical systems, such as divergence (pitchfork bifurcation), single-mode flutter (Hopf bifurcation), coupled-mode flutter (Païdoussis flutter) and restabilization; moreover, the theoretical results can in many cases be validated by relatively easy-to-mount and to-perform experiments. As a result, this problem has been used as a tool for understanding the behaviour of more complex systems, or as a vehicle in the search of new phenomena and new dynamical features.

*Corresponding author at: Department of Hydraulic Engineering, Tsinghua University, Beijing 100084, China. Tel./fax: +86 7348281723.
E-mail address: GuoCQ@hotmail.com (C.Q. Guo).

0889-9746/$ - see front matter © 2010 Elsevier Ltd. All rights reserved.
doi:10.1016/j.jfluidstructs.2010.04.005

In this paper, the focus is on the effects of the fluid viscosity on the governing equation of motion of pipes conveying fluid and on the critical velocities for both divergence and flutter. Although one possible effect of the fluid viscosity, the friction, has been considered in the derivation of the governing equation of motion, another one, the non-uniformity of the flow velocity distribution has been ignored to date.

2. Modification of the centrifugal force term of the equation of motion of the fluid-conveying pipe

The simplest form of a linear differential equation of motion of pipes conveying fluid is given by (see, e.g., Benjamin, 1961a; Gregory and Païdoussis, 1966; Païdoussis and Issid, 1974; Païdoussis 1998, 2005, 2008)

$$EI\frac{\partial^4 w}{\partial x^4}+MU^2\frac{\partial^2 w}{\partial x^2}+2MU\frac{\partial^2 w}{\partial x\partial t}+(M+m)\frac{\partial^2 w}{\partial t^2}=0, \tag{1}$$

where EI is the flexural rigidity of the pipe, M the mass of fluid per unit length, m the mass of the pipe per unit length, U the mean flow velocity and $w=w(x,t)$ the transverse displacement of the pipe at the axial coordinate x and time t.

The dimensionless form of Eq. (1) can be written as

$$\frac{\partial^4 \eta}{\partial \xi^4}+\upsilon^2\frac{\partial^2 \eta}{\partial \xi^2}+2\upsilon\sqrt{\beta}\frac{\partial^2 \eta}{\partial \xi\partial \tau}+\frac{\partial^2 \eta}{\partial \tau^2}=0, \tag{2}$$

by defining the dimensionless variables and parameters

$$\eta=\frac{w}{L},\quad \xi=\frac{x}{L},\quad \tau=\sqrt{\frac{EI}{M+m}}\frac{t}{L^2},\quad \beta=\frac{M}{M+m},\quad \upsilon=\sqrt{\frac{M}{EI}}LU \tag{3}$$

where L is the pipe length, β the mass ratio and υ the dimensionless flow velocity.

Sequentially, the terms in Eq. (1) are associated with: flexural restoring forces, centrifugal forces of the fluid caused by the curvature of the pipe, Coriolis forces of the fluid caused by pipe rotation and inertial forces of the pipe and the internal fluid.

In Eq. (1), gravity, internal damping, a possible elastic foundation, externally imposed tension and pressurization effects are either absent or neglected. If some of these factors are taken into account, more terms will appear in this equation. The interested readers are referred to Païdoussis (2008, Appendix A) for a fuller form of the linear equation of motion. But, however sophisticated the equation may be, the terms in Eq. (1) are the primary ones. For plates and shells in axial flow (see, e.g., Guo and Païdoussis, 2000; Païdoussis, 2004), the equation of motion also has terms similar to those in Eq. (1).

The fluid forces in Eq. (1) are modelled in terms of an ideal-fluid flow (plug flow) model. If a real fluid flow model is to be considered, the viscosity of the fluid may have two effects on the equation: (i) the friction between the fluid and the pipe wall and (ii) the non-uniformity of flow velocity distribution over the cross-section.

The former was first noted and accounted for by Benjamin (1961a) and was later elaborated upon by Païdoussis (1998, 2005, 2008): viscous traction on the pipe and viscous pressure-loss forces exactly cancel out, and hence do not explicitly appear in Eq. (1). In fact, if the pipe and the fluid it conveys are taken as an ensemble, the frictional forces between them are internal forces, and hence should not appear in the equation of motion. As for the latter, some qualitative discussion was provided by Benjamin (1961b), namely that for the MU^2 term, "U^2 would more accurately be interpreted as the average of the squared velocity"; Benjamin then goes on to say that for turbulent pipe flows "the mean square is only 1% or 2% in excess of the square of the mean", and considers it not worthwhile to apply such a small correction. However, nothing was said by Benjamin or anyone else heretofore regarding laminar flows, where the velocity profile is much more different from either that of a plug flow or a fully developed turbulent flow.

In fact, if the non-uniformity of flow velocity distribution is to be considered, the centrifugal force term and the Coriolis force term in Eq. (1) should be calculated for every fluid particle and then integrated over the cross-sectional area. Since the Coriolis force term is a linear function of the flow velocity, integration will yield the same result as in Eq. (1) if U is taken as the mean flow velocity (discharge rate divided by the inner cross-sectional area of the pipe). However, for the centrifugal force term, the result of integration will be greater than that in Eq. (1) because the centrifugal force is a quadratic function of the flow velocity. Therefore, for viscous fluid flow, the coefficient of the second term in Eq. (1) should be taken, instead of MU^2, as $\int_A \rho u^2 \mathrm{d}A$, in which ρ is the fluid density and A the area of the inner cross-section of the pipe. We denote this integral as

$$\int_A \rho u^2 \mathrm{d}A=\alpha MU^2, \tag{4}$$

in which α is the flow-profile-modification factor in the centrifugal force (obviously, for plug flow, $\alpha = 1$). Thus, the modified differential equation of motion of the fluid-conveying pipe takes the form

$$EI\frac{\partial^4 w}{\partial x^4} + \alpha MU^2\frac{\partial^2 w}{\partial x^2} + 2MU\frac{\partial^2 w}{\partial x \partial t} + (M+m)\frac{\partial^2 w}{\partial t^2} = 0, \tag{5}$$

and its dimensionless form becomes

$$\frac{\partial^4 \eta}{\partial \xi^4} + \alpha \upsilon^2 \frac{\partial^2 \eta}{\partial \xi^2} + 2\upsilon\sqrt{\beta}\frac{\partial^2 \eta}{\partial \xi\, \partial \tau} + \frac{\partial^2 \eta}{\partial \tau^2} = 0. \tag{6}$$

3. Flow-profile-modification factors with different flow profiles

3.1. Laminar flow in circular pipe

When the Reynolds number Re < 2300, the flow in a circular pipe is laminar flow (Poiseuille flow), and the flow velocity profile is represented by the well-known parabolic formula (see, e.g., Streeter et al., 1998)

$$u(r) = u_{\max}\left[1 - \left(\frac{r}{R}\right)^2\right], \tag{7}$$

where R is the inner radius of the pipe, r the distance from the fluid particle to the centreline of the pipe and $u_{\max}$ the maximum flow velocity at the centre of the pipe.

If we still use U to denote the mean flow velocity in the pipe, then we have

$$U = \frac{1}{A}\int_A u \mathrm{d}A = \frac{1}{\pi R^2} 2\pi \int_0^R u_{\max}\left[1 - \left(\frac{r}{R}\right)^2\right] r \mathrm{d}r = \frac{1}{2}u_{\max}, \tag{8}$$

and

$$\int_A \rho u^2 \mathrm{d}A = 2\pi \int_0^R \rho u_{\max}^2 \left[1 - \left(\frac{r}{R}\right)^2\right]^2 r \mathrm{d}r = \frac{1}{3}\pi R^2 \rho u_{\max}^2 = \frac{4}{3}MU^2. \tag{9}$$

Therefore, $\alpha = \dfrac{4}{3} \approx 1.333$.

3.2. Turbulent flow in circular pipe

When the Reynolds number Re > 2300, the flow in a circular pipe may become turbulent, and the flow velocity can be represented as its time-average $\overline{u}$ plus a fluctuation u', i.e.

$$u = \overline{u} + u'; \tag{10}$$

thus

$$\int_A u \mathrm{d}A = \int_A \overline{u} \mathrm{d}A + \int_A u' \mathrm{d}A, \tag{11}$$

$$\int_A u^2 \mathrm{d}A = \int_A \overline{u}^2 \mathrm{d}A + 2\int_A \overline{u}u' \mathrm{d}A + \int_A u'^2 \mathrm{d}A. \tag{12}$$

The time-average of the fluctuating flow velocity at every point in the space is zero. Because of this and the symmetry of the circular cross-section, the spatial-average of the fluctuating flow velocity over the cross-sectional area must be zero at any time. Therefore, the second term on the right-hand side of Eqs. (11) and (12) can be taken as zero. For pipes, the turbulence intensity $I \equiv |u'|/U$ is typically between 1% and 5%, and hence the third term on the right-hand side of Eq. (12) is less than 0.25% of the first term and may be neglected.

In the following, the first-term integrals on the right-hand side of Eqs. (11) and (12) will be evaluated for different laws of turbulent flow velocity profile. We hereafter drop the over-bars of the time-averaged velocities for simplicity.

There have been two laws to describe the turbulent velocity profile: the logarithmic law (log law) and the exponential law (power law), both of which were first proposed in the early 20th century. The log law has been more widely accepted by fluid mechanicians than the power law, while the power law has been more popular with engineers. Thus, when Barenblatt et al. (1997) proposed a new power law, it became surprisingly controversial. The controversy even escalated into fierce arguments between log-law disciples and power-law lovers at several international conferences (White, 2006). A laudable effort to resolve the debate was finally offered by Buschmann and Gad-el-Hak (2003), who analyzed 109 different data sets by both the log and power laws. They concluded that the two laws gave comparable agreement and neither was statistically superior. As neutral observers, we use both laws in the following analyses.

3.2.1. Logarithmic law

The widely accepted time-averaged velocity profile in the intermediate region of turbulent flow is the von Kármán–Prandtl universal log law of the wall (see, e.g., Streeter et al., 1998; White, 2006)

$$\frac{u}{u_*}=\frac{1}{\kappa}\ln\frac{u_* y}{\nu}+B, \tag{13}$$

where $u_*=\sqrt{\tau_w/\rho}$ is the friction velocity, τ_w the wall shear stress ($\tau_w=\Delta pR/2$, Δp is the pressure drop per unit length), y the distance from the wall and ν the fluid kinematic viscosity. The parameters κ (von Kármán's constant) and B are constants. For smooth-wall pipes, Nikuradse's experiments yielded $\kappa\approx 0.40$ and $B\approx 5.5$, but later data correlations use the value $\kappa\approx 0.41$ and $B\approx 5.0$ (see White, 2006), which we shall adopt for use in this paper.

For rough-wall pipes, the velocity profile is given by (White, 2006)

$$\frac{u}{u_*}=\frac{1}{\kappa}\ln\frac{u_* y}{\nu}+B-\frac{1}{\kappa}\ln\left(1+0.3\frac{u_*\varepsilon}{\nu}\right), \tag{14}$$

where ε represents the diameter of sand grains.

By defining the "equivalent" viscosity

$$\nu_e=\nu+0.3u_*\varepsilon, \tag{15}$$

we can rewrite Eq. (14) in the form of Eq. (13)

$$\frac{u}{u_*}=\frac{1}{\kappa}\ln\frac{u_* y}{\nu_e}+B. \tag{16}$$

For circular pipes, both Eqs. (13) and (16) can be represented in terms of the maximum velocity $u_{\max}$ at the centreline $y=R$ in the same form

$$u=u_{\max}+\frac{u_*}{\kappa}\ln\frac{y}{R}. \tag{17}$$

Eqs. (13), (16) and (17) hold in the turbulent zone only. However, the thickness δ of the viscous sub-layer near the wall plus the buffer layer and the flow velocities in these regions are so small that the integration over them can be neglected. Thus, we have

$$U=\frac{1}{A}\int_A u\mathrm{d}A=\frac{1}{\pi R^2}\lim_{\delta\to 0}2\pi\int_0^{R-\delta}ur\mathrm{d}r=\frac{2}{R^2}\lim_{\delta\to 0}\int_\delta^R\left(u_{\max}+\frac{u_*}{\kappa}\ln\frac{y}{R}\right)(R-y)\mathrm{d}y=u_{\max}-\frac{3u_*}{2\kappa}, \tag{18}$$

and

$$\begin{aligned}\int_A\rho u^2\mathrm{d}A&=\lim_{\delta\to 0}2\pi\int_0^{R-\delta}\rho u^2 r\mathrm{d}r=2\pi\rho\lim_{\delta\to 0}\int_\delta^R\left(u_{\max}+\frac{u_*}{\kappa}\ln\frac{y}{R}\right)^2(R-y)\mathrm{d}y\\&=\pi R^2\rho\left(u_{\max}^2-3u_{\max}\frac{u_*}{\kappa}+\frac{7u_*^2}{2\kappa^2}\right)=M\left(U^2+\frac{5u_*^2}{4\kappa^2}\right);\end{aligned} \tag{19}$$

hence

$$\alpha = 1 + \frac{5}{4}\left(\frac{u_*}{\kappa U}\right)^2. \tag{20}$$

What we should note is that the shear velocity u_* is not a constant; it increases with increasing mean velocity U, but is not exactly proportional to it. Typically, U/u_* ranges from 15 to 25. Fig. 1 shows the variation of the flow-profile-modification factor α in this range.

From Eq. (18), we find that

$$\frac{u_*}{\kappa U} = \frac{2}{3}\left(\frac{u_{\max} - U}{U}\right). \tag{21}$$

Substituting into Eq. (20), we obtain an alternate expression for α in terms of U and $u_{\max}$, namely

$$\alpha = 1 + \frac{5}{9}\left(\frac{u_{\max} - U}{U}\right)^2. \tag{22}$$

As aforementioned, we have the same turbulent velocity profile, Eq. (17), in terms of the maximum velocity $u_{\max}$ for both smooth-wall and rough-wall pipes; hence the formulas for calculating the flow-profile-modification factor α, Eqs. (20) and (22), hold for both. This is true because, as White (2006) noted, the outer or defect layer is not affected by wall roughness. However, this does not mean that wall roughness has no effect on α. For a given mean flow velocity U, with increasing wall roughness, the pressure drop Δp, hence the shear stress τ_w and the friction velocity u_* increase, and therefore the flow-profile-modification factor α increases.

3.2.2. *Exponential law*

The time-averaged flow velocity profile can also be expressed according to the exponential law (Streeter et al., 1998)

$$u(r) = u_{\max}\left(\frac{y}{R}\right)^{1/n}, \tag{23}$$

where the exponent n is dependent on the Reynolds number. In the range $\mathrm{Re} = 3 \times 10^3$–$10^5$, $n = 7$ for smooth-wall circular pipes, which is the well-known $\frac{1}{7}$ exponential law developed by Prandtl based on Nikuradse's experimental data, and $n = 4$–5 for rough-wall circular pipes.

Then the mean flow velocity in the pipe is

$$U = \frac{1}{A}\int_A u\mathrm{d}A = \frac{1}{\pi R^2}2\pi\int_0^R u r\mathrm{d}r = \frac{2}{R^2}\int_0^R u_{\max}\left(\frac{y}{R}\right)^{1/n}(R-y)\mathrm{d}y = \frac{2n^2}{(2n+1)(n+1)}u_{\max}, \tag{24}$$

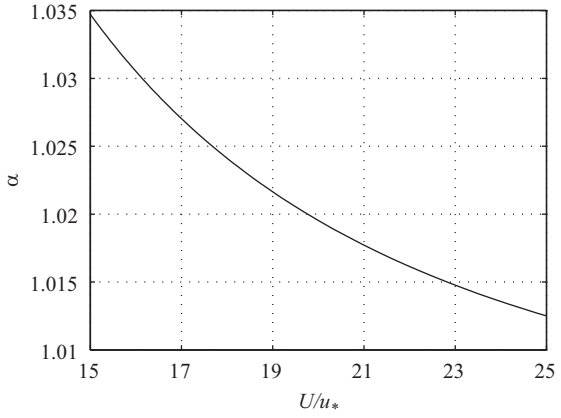

Fig. 1. Flow-profile-modification factor α versus U/u_* with the turbulent log law.

and the integral $\int_A \rho u^2 \mathrm{d}A$ becomes

$$\int_A \rho u^2 \mathrm{d}A = 2\pi\rho \int_0^R u^2 r \mathrm{d}r = 2\pi\rho \int_0^R u_{\max}^2 \left(\frac{y}{R}\right)^{2/n} (R-y)\mathrm{d}y = \pi R^2 \rho \frac{n^2}{(n+1)(n+2)} u_{\max}^2. \tag{25}$$

Therefore

$$\alpha = \frac{1}{MU^2}\int_A \rho u^2 \mathrm{d}A = \frac{(2n+1)^2(n+1)}{(2n)^2(n+2)} = 1 + \frac{5n+1}{(2n)^2(n+2)}. \tag{26}$$

For $n = 7$, $\alpha \approx 1.020$; and for $n = 4$–5, $\alpha \approx 1.037$–1.055.

The flow-profile-modification factor α variation with the exponent n is shown in Fig. 2. It decreases monotonically with increasing n.

More recently, Barenblatt et al. (1997) proposed a more detailed power law, which is also based on Nikuradse's experiments

$$\frac{u}{u_*} = \left(\frac{1}{\sqrt{3}}\ln \mathrm{Re} + \frac{5}{2}\right)\left(\frac{u_* y}{\nu}\right)^{3/(2\ln \mathrm{Re})}. \tag{27}$$

Expressing it in terms of $u_{\max}$, we get

$$u(r) = u_{\max}\left(\frac{y}{R}\right)^{3/(2\ln \mathrm{Re})}. \tag{28}$$

It is almost the same as Prandtl's power law, except that the exponent n is specified as a function of the Reynolds number

$$n = \frac{2}{3}\ln \mathrm{Re}. \tag{29}$$

The solid line in Fig. 3 shows the variation of the flow-profile-modification factor α with Reynolds number according to the new power law using a logarithmic abscissa.

To compare with the log law, we should first find the relation between U/u_* in Eq. (20) and the Reynolds number $\mathrm{Re} = U(2R)/\nu$. From Eq. (13), we have

$$\frac{u_{\max}}{u_*} = \frac{1}{\kappa}\ln\frac{u_* R}{\nu} + B = \frac{1}{\kappa}\ln\frac{u_* \mathrm{Re}}{2U} + B. \tag{30}$$

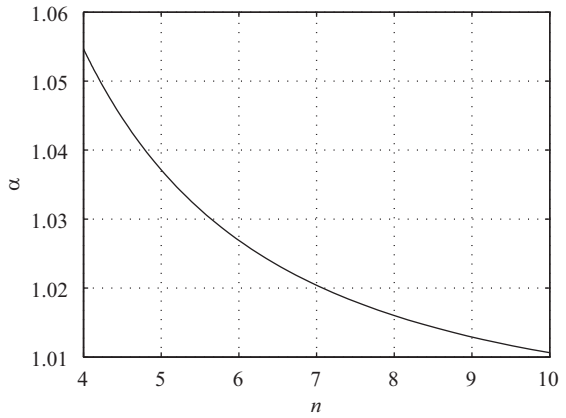

Fig. 2. Flow-profile-modification factor α versus the exponent n with Prandtl's turbulent power law.

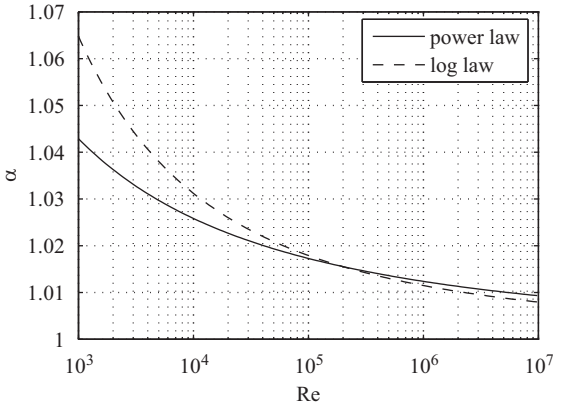

Fig. 3. Flow-profile-modification factor α versus Reynolds number with the turbulent power law by Barenblatt et al. (1997), comparing with the log law.

Substituting Eq. (18) into to Eq. (30), we can express the Reynolds number in terms of U/u_*

$$\mathrm{Re} = 2\frac{U}{u_*}\exp\left[\kappa\left(\frac{U}{u_*} - B\right) + \frac{3}{2}\right]. \tag{31}$$

With Eqs. (20) and (31), we can plot the log-law α–Re curve with U/u_* as the parameter, which is shown in Fig. 3 by the dashed line. In the range $\mathrm{Re} > 10^4$, the results given by both the power law and the log law are in fairly good agreement with each other.

In Eqs. (27)–(31), the Reynolds number is defined in the case of a smooth-wall circular pipe as $\mathrm{Re} = U(2R)/\nu$. For rough-wall pipes, the viscosity ν in this definition should be replaced by the "equivalent" viscosity ν_e (Monin and Yaglom, 1975; Barenblatt et al., 1997); hence

$$\mathrm{Re} = \frac{2RU}{\nu_e} = \frac{2RU}{\nu + 0.3u_*\varepsilon} \approx \frac{2RU}{0.3u_*\varepsilon} \sim 100\frac{R}{\varepsilon}. \tag{32}$$

From the above analyses, we conclude, for turbulent flow, that: (i) the log law and power low give results in fairly good agreement with each other for the flow-profile-modification factor α; (ii) α decreases with increasing Reynolds number Re for both smooth-wall and rough-wall pipes; (iii) in the range $\mathrm{Re} = 3\times10^3$–$3\times10^5$, we have $\alpha = 1.015$–1.040 for smooth-wall circular pipes, and $\alpha = 1.035$–1.055 for rough-wall circular pipes.

4. Equivalent flow velocity and equivalent mass

Define the equivalent flow velocity

$$\tilde{U} = \alpha U, \tag{33}$$

and the equivalent masses

$$\tilde{M} = \frac{M}{\alpha}, \quad (\tilde{M} + \tilde{m}) = (M + m). \tag{34}$$

Then Eqs. (5) and (6) can be rewritten as

$$EI\frac{\partial^4 w}{\partial x^4} + \tilde{M}\tilde{U}^2\frac{\partial^2 w}{\partial x^2} + 2\tilde{M}\tilde{U}\frac{\partial^2 w}{\partial x\partial t} + (\tilde{M} + \tilde{m})\frac{\partial^2 w}{\partial t^2} = 0, \tag{35}$$

and

$$\frac{\partial^4 \eta}{\partial \xi^4} + \tilde{v}^2\frac{\partial^2 \eta}{\partial \xi^2} + 2\tilde{v}\sqrt{\tilde{\beta}}\frac{\partial^2 \eta}{\partial \xi\partial \tau} + \frac{\partial^2 \eta}{\partial \tau^2} = 0, \tag{36}$$

respectively, where

$$\tilde{\upsilon} = \sqrt{\frac{\tilde{M}}{EI}} L\tilde{U} = \sqrt{\alpha}\sqrt{\frac{M}{EI}} LU = \sqrt{\alpha}\upsilon \tag{37}$$

is the equivalent dimensionless flow velocity, and

$$\tilde{\beta} = \frac{\tilde{M}}{\tilde{M}+\tilde{m}} = \frac{M}{\alpha(M+m)} = \frac{\beta}{\alpha} \tag{38}$$

is the equivalent mass ratio.

Comparing Eqs. (35) and (36) with Eqs. (1) and (2), it can easily be seen that they have identical form. By substituting $\tilde{U}$, $\tilde{M}$ and $\tilde{M}+\tilde{m}$ in Eq. (35) with U, M and $M+m$, and $\tilde{\upsilon}$, $\tilde{\beta}$ in Eq. (36) with υ and β, we get Eq. (1) and Eq. (2), respectively. Therefore, problems involving pipes conveying fluid with different flow profiles can be solved with the equations of motion for plug flow. The only thing to be done is to replace the flow velocity and the masses with the equivalent flow velocity and the equivalent masses defined in Eqs. (33) and (34), or the dimensionless flow velocity and the mass ratio with their corresponding equivalents defined in Eqs. (37) and (38).

In the new terminology of 'equivalent flow velocity', 'equivalent mass', 'equivalent dimensionless flow velocity' and 'equivalent mass ratio' coined in this paper, by 'equivalent' we mean 'equivalent to that of plug flow'.

It should be noted that, in rescaling Eqs. (5) and (6) to Eqs. (35) and (36), the relations defined in Eqs. (33), (34), (37) and (38) are velocity dependent because the parameter α is Reynolds number dependent.

In all forms of the equation of motion of pipes conveying fluid, from the simplest ones as given in Eqs.(1) and (2) to more complicated nonlinear ones (see, e.g., Païdoussis, 2008, Appendix B), the flow velocity and masses appear in the dimensionless equations only in the forms of υ^2 and $\upsilon\sqrt{\beta}$, therefore, the modification and the rescaling introduced in this section can be applied to all of them.

For other problems of axial-flow induced vibrations, such as with axial external flow along a cylinder (see, e.g., Lopes et al., 2002), the effect of the non-uniform velocity profile of the flow can also be taken into consideration by similar modification on the equations of motion. However, the rescaling introduced in this section cannot be applied to them, because there exist terms involving the flow velocity and masses in the dimensionless equations other than in the forms of υ^2 and $\upsilon\sqrt{\beta}$.

5. Critical flow velocities for pipes conveying fluid for different flow profiles

5.1. Critical flow velocities for divergence

It has been known for a long time (e.g., Housner, 1952) that, for positively supported (with clamped or pinned supports at both ends) pipes conveying fluid, when the flow velocity reaches some critical point, the pipe loses stability statically by divergence, i.e., it buckles. This has been confirmed by experiments, by Dodds and Runyan (1965) and others. At this point, the vibrations of the pipe disappear, and the time-dependent terms in the equation of motion vanish; then Eq. (35) reduces to one similar to the critical equilibrium equation of a column subject to an axial compressive force. The equivalent critical flow velocity and the dimensionless equivalent critical flow velocity for divergence of the fluid-conveying pipe are given by

$$\tilde{U}_{cd} = \frac{\pi}{\mu L}\sqrt{\frac{EI}{\tilde{M}}}, \quad \tilde{\upsilon}_{cd} = \frac{\pi}{\mu}, \tag{39}$$

where μ is the length coefficient, which is related to the type of end supports of the pipe. For simply supported pipes, $\mu = 1$; for pipes clamped at both ends, $\mu = 0.5$. From Eqs. (33), (34), (37) and (39), we can obtain the critical flow velocity and the dimensionless critical flow velocity for divergence

$$U_{cd} = \frac{\pi}{\mu L}\sqrt{\frac{EI}{\alpha M}}, \quad \upsilon_{cd} = \frac{\pi}{\mu\sqrt{\alpha},} \tag{40}$$

both of which are $1/\sqrt{\alpha}$ times that with plug flow.

By substituting the previously obtained α into Eq. (40), the critical flow velocities for divergence can be calculated in the cases of laminar flow in circular pipes, turbulent flow in smooth-wall circular pipes, and turbulent flow in rough-wall circular pipes, which are found to be 13.4%, 0.74–1.9%, and 1.7–2.6%, respectively, *lower* than that with plug flow.

5.2. Critical flow velocities for flutter

It is known that fluid-conveying cantilevers are nonconservative in nature, and no divergence can occur. Instead, they lose stability by single-mode flutter (Gregory and Païdoussis, 1966; Chen, 1987; Païdoussis and Li, 1993; Païdoussis, 1970, 1998, 2008). By employing the Galerkin approach to approximate the partial differential equation of motion as a finite set of coupled ordinary differential equations and solving for the eigenvalues of its coefficient matrix, the critical flow velocity for flutter can be obtained.

Take Eq. (6) as an example, and let

$$\eta(\xi,\tau)=\sum_{i=1}^{N}\psi_i(\xi)T_i(\tau), \tag{41}$$

where $\psi_i(\xi)$ is the ith normalized *in vacuo* beam eigenfunction for a cantilever. Multiplying Eq. (6) by $\psi_j(\xi)$, and integrating with respect to ξ along [0,1], we have

$$T_j'' = -\lambda_j^4 T_j - \alpha v^2 \sum_{i=1}^{N} T_i \int_0^1 \psi_i'' \psi_j \mathrm{d}\xi - 2v\sqrt{\beta}\sum_{i=1}^{N} T_i' \int_0^1 \psi_i' \psi_j \mathrm{d}\xi_i, \quad (j=1,2,\cdots,N), \tag{42}$$

in which the orthogonality of the beam eigenfunctions has been accounted for. Eq. (42) represents a set of second-order ordinary differential equations. In order to solve it by standard procedures, we reduce it to first order by letting

$$\mathbf{z}=[T_1 \quad \cdots \quad T_n \quad T_1' \quad T_n']^{\mathrm{T}}; \tag{43}$$

thus, Eq. (42) is transformed to a set of first-order ordinary differential equations with $2n$ variables

$$\mathbf{z}'=\mathbf{C}\mathbf{z}. \tag{44}$$

The condition for the pipe to flutter is that the coefficient matrix $\mathbf{C}$ of Eq. (44) has at least one eigenvalue with non-negative real part.

In Fig. 4 are shown the results calculated with $N=10$ for the dimensionless critical flow velocities for flutter varying with the mass ratio for different flow profiles. The curve for plug flow (solid line) is the same as that given in Païdoussis (1998). The S-shaped segments are associated with the sequence for the pipe to first lose stability by flutter, then regain it, and finally lose it again (according to linear theory), as the flow velocity increases. The negative-slope portions of the curves correspond to the thresholds of restabilization.

For plug flow ($\alpha=1$), it is well known that, as $\beta\to 1$, more and more beam modes participate in the dynamics, hence the results are sensitive to N. For laminar flow ($\alpha=1.333$), however, the maximum difference between the critical flow velocity obtained with $N=10$ and that with $N=20$ is found to be less than 0.1%. The reason is that, according to Eq. (38), $\alpha=1.333$, $\beta=1$ is equivalent to $\alpha=1$, $\beta=0.75$ (both have the same equivalent mass ratio $\beta=0.75$); that is, $\beta=1$ for laminar flow is at the same level of sensitivity to N as $\beta=0.75$ for plug flow.

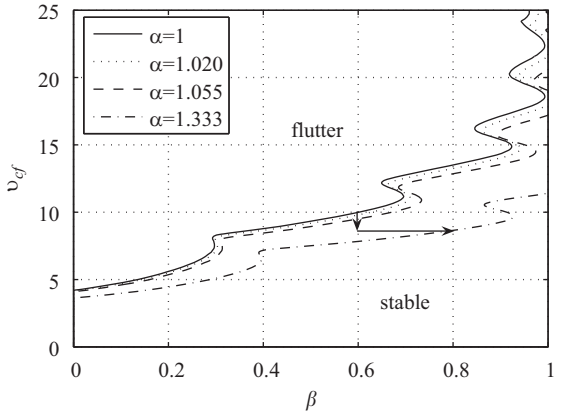

Fig. 4. Dimensionless critical flow velocities v_{cf} for flutter versus mass ratio β for cantilevered pipes conveying fluid with different flow profiles.

In Fig. 4 it can be seen that the dimensionless critical flow velocity v_{cf} decreases with increasing flow-profile-modification factor α for a given mass ratio β. The rate of decrease of v_{cf} in a particular curve compared with that for plug flow is not a constant. It depends on β, but does not change monotonically as β increases. When $\beta = 0.8$, the decrease of the critical flow velocity for laminar flow ($v_{cf} = 8.65$) compared with that for plug flow ($v_{cf} = 13.50$) is as high as 36%!

Another significant phenomenon revealed by Fig. 4 is that as $\beta \to 1$, while a plug flow model predicts an infinite critical flow velocity, i.e., no flutter may occur, real-fluid models predict finite ones, i.e., flutter is possible!

By using the concepts of equivalent flow velocity and equivalent mass ratio defined in Eqs. (37) and (38), we only need to calculate for the solid line with plug flow ($\alpha = 1$), because it also represents the $\tilde{v}_{cf}$ versus β relation for all flow profiles. Those with other flow profiles can be obtained by compressing this curve downwards to $1/\sqrt{\alpha}$ times in height and stretching it rightwards to α times in width, with the coordinate axes unmoved. For instance, for laminar flow ($\alpha = 1.333$), when $\beta = 0.8$, $\tilde{\beta} = \beta/\alpha = 0.6$, the solid line gives $\tilde{v}_{cf} \approx 9.99$; thus, $v_{cf} = \tilde{v}_{cf}/\sqrt{\alpha} \approx 8.65$. The processes of compression and stretching are shown by the two arrows in Fig. 4. Since overall the curve is ascending, both the vertical compression and the horizontal stretching reduce the critical flow velocity for a given β. Hence, flow profiles have an even greater effect on the critical flow velocity for flutter than that they do for divergence, in which case the stretching has no effect because $\tilde{v}_{cd}$ is independent of $\tilde{\beta}$, and therefore $\tilde{v}_{cd}-\tilde{\beta}$ would be a horizontal line.

It is the flow velocity profile in the pipe cross-section that directly affects the equation of motion and the critical flow velocities of fluid-conveying pipes, while the flow velocity profile depends only on the flow type and is not explicitly related to the viscosity coefficient. The viscosity coefficient plays an implicit role via the Reynolds number, which determines the flow type.

6. Conclusions

The effects of the non-uniformity of the flow velocity distribution of the real fluid on the equation of motion for fluid-conveying pipes have been ignored to date. In this paper, the centrifugal force term in the equation of motion is modified by first calculating the centrifugal force for every fluid particle with different flow profiles, and then integrating over the cross-sectional area. The flow-profile-modification factors are found to be 1.333, 1.015–1.040 and 1.035–1.055 for laminar flow in circular pipes, turbulent flow in smooth-wall circular pipes and turbulent flow in rough-wall circular pipes, respectively. The critical flow velocities for divergence in the above-mentioned three cases are found to be 13.4%, 0.74–1.9% and 1.7–2.6%, respectively, *lower* than with plug flow; those for flutter are even lower, and could reach 36% for the laminar flow profile in the case of $\beta = 0.8$. By introducing two new concepts of equivalent flow velocity and equivalent mass, fluid-conveying pipe problems with different flow profiles can be solved with the equation of motion for plug flow. The effects of fluid viscosity on the equation of motion and the critical flow velocity of a fluid-conveying pipe are explicitly related only to the flow profile.

Particularly significant are the results for laminar flow, especially in conjunction with applications in MEMS; see, for instance, Rinaldi et al. (2010).

Acknowledgement

The first author wishes to acknowledge with gratitude the instructive consultations on turbulent flow with Prof. Z. J. Wang and Dr Y. Zhou, Department of Aerospace Engineering, Iowa State University, USA.

References

Ashley, H., Haviland, G., 1950. Bending vibration of pipe line containing flowing fluid. Journal of Applied Mechanics 17 (3), 229–232.

Barenblatt, G.I., Chorin, A.J., Prostokishin, V.M., 1997. Scaling laws for fully developed turbulent flow in pipes: discussion of experimental data. Proceedings of the National Academy of Sciences of the United States 94, 773–776.

Benjamin, T.B., 1961a. Dynamics of a system of articulated pipes conveying fluid, I theory. Proceedings of the Royal Society A261 (130), 457–486.

Benjamin, T.B., 1961b. Dynamics of a system of articulated pipes conveying fluid, II experiments. Proceedings of the Royal Society A261 (130), 487–499.

Buschmann, M.H., Gad-el-Hak, M., 2003. Debate concerning the mean-velocity profile of a turbulent boundary layer. AIAA Journal 41 (4), 565–572.

Chen, S.S., 1987. In: Flow-induced Vibration of Circular Cylindrical Structures. Hemisphere Publishing Corporation, Washington.
Dodds Jr., H.L., Runyan, H.L., 1965. Effect of high velocity fluid flow on the bending vibrations and static divergence of a simply supported pipe. NASA Technical Note, D–2870.
Gregory, R.W., Païdoussis, M.P., 1966. Unstable oscillation of tubular cantilevers conveying fluid, I theory. Proceedings of the Royal Society A293 (1435), 512–527.
Guo, C.Q., Païdoussis, M.P., 2000. Stability of rectangular plates with free side-edges in two-dimensional inviscid channel flow. Journal of Applied Mechanics 67 (1), 171–176.
Housner, G.W., 1952. Bending vibrations of a pipe line containing flowing fluid. Journal of Applied Mechanics 19 (2), 205–208.
Lopes, J.-L., Païdoussis, M.P., Semler, C., 2002. Linear and nonlinear dynamics of cantilevered cylinders in axial flow, Part 2: the equations of motion. Journal of Fluids and Structures 16 (6), 715–737.
Monin, A.S., Yaglom, A.M., 1975. Statistical Fluid Mechanics, Vol. 1. MIT Press, Boston.
Païdoussis, M.P., 1970. Dynamics of tubular cantilevers conveying fluid. Journal of Mechanical Engineering Science 12, 85–103.
Païdoussis, M.P., Issid, N.T., 1974. Dynamic stability of pipes conveying fluid. Journal of Sound and Vibration 33 (3), 267–294.
Païdoussis, M.P., Li, G.X., 1993. Pipes conveying fluid, a model dynamical problem. Journal of Fluids and Structures 7 (2), 137–204.
Païdoussis, M.P., 1998. Fluid–Structure Interactions: Slender Structures and Axial Flow, Vol. 1. Academic Press, London.
Païdoussis, M.P., 2004. Fluid–Structure Interactions: Slender Structures and Axial Flow, Vol. 2. Elsevier Academic Press, London.
Païdoussis, M.P., 2005. Some unresolved issues in fluid-structure interactions. Journal of Fluids and Structures 20 (3), 871–890.
Païdoussis, M.P., 2008. The canonical problem of the fluid-conveying pipe and radiation of the knowledge gained to other dynamics problems across Applied Mechanics. Journal of Sound and Vibration 310 (3), 462–492.
Rinaldi, S., Prabhakar, S., Vengallatore, S., Païdoussis, M.P., 2010. Dynamics of microscale pipes containing internal fluid flow: damping, frequency shift, and stability. Journal of Sound and Vibration 329 (8), 1081–1088.
Streeter, V.L., Wylie, E.B., Bedford, K.W., 1998. In: Fluid Dynamics 9th edition McGraw-Hill, New York.
White, F.M., 2006. In: Viscous Fluid Flow 3rd edition McGraw-Hill, New York.